Inorg. Chem. **2007**, *46*, 446–452

Phase Transition in Tl_2TeO_3: Influence and Origin of the Thallium Lone Pair Distortion

Franziska Rieger and Anja-Verena Mudring*

Anorganische Chemie I, Ruhr-Universität Bochum, Universitätsstrasse 150, D-44801 Bochum, Germany, and Department of Chemistry, Iowa State University, Ames, Iowa 50010

Received July 10, 2006

A new modification of thallium tellurite, β-Tl_2TeO_3, has been synthesized by methanolothermal reaction, and its phase transition has been studied by single-crystal X-ray diffraction. At a temperature of 440(10) °C an irreversible phase transition from a monoclinic structure (β-Tl_2TeO_3: $P2_1/c$ (No. 14), $Z = 4$, $a = 8.9752(18)$ Å, $b = 4.8534(6)$ Å, $c = 11.884(2)$ Å, $\beta = 109.67(2)°$, $V = 487.47(15)$ Å^3 at 25 °C) to an orthorhombic structure (α-Tl_2TeO_3: *Pban* (No. 50), $Z = 8$, $a = 16.646(2)$ Å, $b = 11.094(2)$ Å, $c = 5.2417(8)$ Å, $V = 968.0(3)$ Å^3 at 25 °C) is observed. Both structures are characterized by ψ-tetrahedral TeO_3^{2-} anions. In the orthorhombic structure ψ-trigonal bipyramidal [TlO_4] units are found together with ψ-tetrahedral [TlO_3] units whereas in the monoclinic structure the coordination polyhedron around Tl(I) can be best described as a ψ-square pyramide, ψ-[TlO_4]. The electronic structure of Tl_2TeO_3 in both modifications has been studied to explain the influence of the lone pairs. It can be conclusively shown that the minimization of antibonding *n*s-metal/2p-oxygen interactions is the driving force for "lone pair" distortions which determines the structures of Tl_2TeO_3.

Introduction

The oxotellurite class shows a wide variety of structures. Compounds of the composition M_2TeO_3 with M = Li, Na, K, Rb, Cs, Tl, and Ag or $MTeO_3$ with Mg, Sr, Ba, Pb, Mn, Co, Ni, Cu, Zn, Cd, Hg, and UO^{2+} with the ψ-tetrahedral anion TeO_3^{2-} are well-known.[1] Other compounds containing this complex anion are $Fe_2Te_3O_9$,[2] Fe_2TeO_5,[3] and $Co_6(TeO_3)_4(TeO_4)$.[5] Furthermore, higher condensed anionic units such as $Te_2O_5^{2-}$ (dimers) in, e.g., $MnTe_2O_5$[6] or $Te_3O_8^{4-}$ (trimers, CN of 3 and 4 around tellurium) in, e.g., $Zn_2Te_3O_8$[7] and $Te_4O_9^{4-}$ (tetramers) in $Cs_2Te_4O_9$[8] have been described. The orthotellurite(IV) anion TeO_4^{4-}, a ψ-square pyramid, has been observed in $Co_6Te_5O_{16}$.[9] Tellurites can even form open framework structures as in $KGaTe_2O_6 \cdot 1.8H_2O$.[10] All structures of tellurites(IV) have in common that they are influenced by the stereochemical activity of the $5s^2$ lone pair on tellurium.

With this lone pair many interesting material properties have been associated. The ψ-tetrahedral MO_3 units may give rise to nonsymmetric space groups,[11] which is a prerequisite for many material relevant physical properties to occur as,

* To whom correspondence should be addressed at the Universität zu Köln. E-mail: anja.mudring@rub.de. Web: http://www.anjamudring.de.

(1) Kohn, K.; Inoue, K.; Horie, O.; Akimoto, S. *J. Solid State Chem.* **1976**, *18*, 27. Loopstra, B. O.; Brandenburg, N. P. *Acta Crystallogr.* **1978**, *34*, 1335. Folger, F. *Z. Anorg. Allg. Chem.* **1975**, *411*, 103. Folger, F. *Z. Anorg. Allg. Chem.* **1975**, *411*, 111. Kocak, M.; Platte, C.; Troemel, M. *Z. Anorg. Allg. Chem.* **1979**, *453*, 93. Lindqvist, O. *Acta Chem. Scand.* **1972**, *26*, 1423. Hanke, K. *Naturwissenschaften* **1967**, *54*, 199. Mariolacos, K. *Anz. Oesterr. Akad. Wiss. Math.-Naturwiss. Kl.* **1969**, *106*, 129. Philippot, E.; Maurin, M. *Rev. Chim. Miner.* **1976**, *13*, 162. Thuemmel, H. J.; Hoppe, R. *Z. Naturforsch., B* **1974**, *29*, 28. Kuban, R. J. *Cryst. Res. Technol.* **1983**, *18*, 85. Loopstra, B. O.; Goubitz, B. O. K. *Acta Crystallogr.* **1986**, *C42*, 520. Kraemer, V.; Brandt, G. *Acta Crystallogr.* **1985**, *C41*, 1152. Sciau, P.; Lapasset, J.; Moret, J. *Acta Crystallogr.* **1986**, *42*, 1688. Kraemer, V.; Brandt, G. *Acta Crystallogr.* **1986**, *42*, 917. Andersen, L.; Langer, V.; Stroemberg, A.; Stroemberg, D. *Acta Crystallogr.* **1989**, *45*, 344. Elerman, Y. *Phase Transitions* **1992**, *8*, 127. Masse, R.; Guitel, J. C.; Trodjman, I. *Mater. Res. Bull.* **1980**, *15*, 431. Frit, B.; Mercurio, D. *Rev. Chim. Miner.* **1980**, *17*, 192. Pertlik, F. *J. Solid State Chem.* **1987**, *71*, 291. Grice, J. D. *Can. Mineral.* **1989**, *27*, 133. Frit, B.; Mercurio, D.; Thomas, P.; Champarnaud-Mesjard, J. C. *Z. Kristallogr. New Cryst. Struct.* **1999**, *214*, 439.

(2) Astier, R.; Philippot, E. Moret, J.; Maurin, M. *Rev. Chim. Miner.* **1976**, *13*, 359.
(3) Jumas, J. C.; Wintenberger, M.; Philippot, E. *Mater. Res. Bull.* **1977**, *12*, 1063.
(4) Weber, F. A.; Schleid, T. *Z. Anorg. Allg. Chem.* **2000**, *626*, 1285.
(5) Troemel, M.; Scheller, T. *Z. Anorg. Allg. Chem.* **1976**, *427*, 229.
(6) Walitzi, E. M. *Naturwissenschaften* **1964**, *51*, 334.
(7) Hanke, K. *Naturwissenschaften* **1966**, *53*, 273.
(8) Loopstra, B. O.; Goubitz, K. *Acta Crystallogr.* **1986**, *C42*, 520.
(9) Troemel, M.; Scheller, T. *Naturwissenschaften* **1973**, *60*, 103.
(10) Ok, K. M.; Halasyamani, P.S. *Chem. Mater.* **2001**, *13*, 4278.
(11) See for example: Xiao, D. R.; An, H. Y.; Wang, E. B.; Xu, L. Hu, C. W. *J. Mol. Struct.* **2005**, *733*, 69.

10.1021/ic061273j CCC: $37.00
Published on Web 12/15/2006

for example, the potential use as second-harmonic-generating (SHG) materials.[12] Experimental studies have shown that the local surrounding of tellurium by oxygen atoms in the form of a ψ-trigonal bipyramid in TeO_2 glasses is similar to that in crystalline TeO_2.[13] Upon addition of glass modifiers the local surrounding changes gradually to a ψ-tetrahedron.[14] The applications of tellurite glasses based mostly on their nonlinear optical properties and wide infrared spectral transmittance range from optical modulators, memories, windows for IR transmission, and bonding materials in magnetic heads to optical fibers and fiber amplifiers.[15]

Theoretical analyses indeed confirm that the lone pair of electrons on the tellurium atom is the key to the nonlinear optical properties of the TeO_2-based glasses and that TeO_4 units rather than TeO_3 units are responsible for this effect.[16] All of these lone pair based effects should be even more pronounced when a second ion with a lone pair like that of Tl(I) is combined with Te(IV).[17] Indeed, it is well-established that thallium tellurite glasses have interesting properties. They exhibit for example zero material dispersion wavelengths (ZMDWs) over 2.2 μm.[18] $Tl_2O/Bi_2O_3/SiO_2$ glasses show an exceptionally high nonlinear refractive index.[19]

Although the "stereochemical" active lone pair determines many of the physical properties of these materials, its origin and true nature has not yet been conclusively established. We were recently able to show that structural distortions in thallium coordination compounds which traditionally would be attributed to a stereochemically active lone pair do not originate from a s−p hybridization on the thallium(I) cation to give the lone pair a structural directionality but from the tendency to minimize unfavorable *anti*-bonding interactions of the $6s^2$ electron pair of thallium with its bonding partner. To investigate the lone pair effect in solid materials, we have synthesized monoclinic Tl_2TeO_3, studied its phase transition, and, additionally, carried out calculations on the basis of density functional theory on the different modifications.

(12) Halasyamani, P. S. *Angew. Chem., Int. Ed.* **2004**, *43*, 5489.
(13) Neov, S.; Gerasimova, I.; Kozhukarov, V.; Marinov. M. *J. Mater. Sci.* **1980**, *15*, 1153.
(14) Hao, J.; Lam, D.; Sigel G. H.; Mendoza, E. A., Jr.; Hensley, D. A. *J. Am. Ceram. Soc.* **1992**, *75*, 277. Jiang, N.; Spencer, J. C. H. *Phys. Rev. B* **2004**, 184113.
(15) El-Mallawany, R. A. H. *Tellurite Glasses: Physical Properties and Data*; CRC Press: Boca Raton, FL, 2002.
(16) Suehara, S.; Thomas, P.; Mirgorodsky, A.; Merle-Méjean, T.; Champarnaud-Mesjard, J. C.; Aizawa, T.; Shishita, S. Todoroki, T. Konishi, S. Inoue *J. Non-Cryst. Solids* **2004**, *345*, 730. Suehara, S.; Thomas, P.; Mirgorodsky, A.; Merle-Meiean, T.; Champarnaud-Mesjard, J. C.; Aizawa, T.; Shishita, S.; Todoroki, T.; Konishi, S.; Inoue. *Phys. Rev. B* **2004**, 5840.
(17) Jeansannetas, B.; Blanchandin, S.; Thomas, P.; Marchet, P.; Champarnaud-Mesjard, J. C.; Merle-Méjean, T.; Frit, B.; Nazabal, V.; Fargin, E.; LeFlem, G.; Martin, M. O.; Bousquet, B.; Canioni, L.; Le Boiteux, S.; Segonds, P.; Sarger, L. *J. Solid State Chem.* **1999**, *146*, 329. Noguera, O.; Merle-Méjean, T.; Mirogordosky, A. P.; Thomas, P.; Champarnaud-Mesjard, J. C. *J. Non-Cryst. Solids* **2003**, *330* (1−3), 50−60. Vrillet, G.; Thomas, P.; Couderc, V.; Barthélémy, A.; Champardnaud-Mesjard, J.-C. *J. Non-Cryst. Solids* **2004**, *345*, *346*, 417.
(18) Mito, T.; Fujino, S.; Takebe, H.; Morinaga, K.; Todoroki, S.; Sakaguchi, S. *J. Non-Cryst. Solids* **1997**, *210*, 155.
(19) Kim, S. H.; Yoko, T.; Sakka, S. *J. Am. Ceram. Soc.* **1993**, *76*, 1061 Jeansannetas, B.; Blanchandin, S.; Thomas, P.; Marchet, P; Champarnaud-Mesjard, J. C.; Merle-Méjean, T.; Frit, B.; Nazabal, V.; Fargin, E.; Le Flem, G.; Martin, M. O.; Bousquet, B.; Canioni, L.; Le Boiteux, S.; Segonds, P.; Sarger, L. *J. Solid State Chem.* **1999**, *146*, 329.

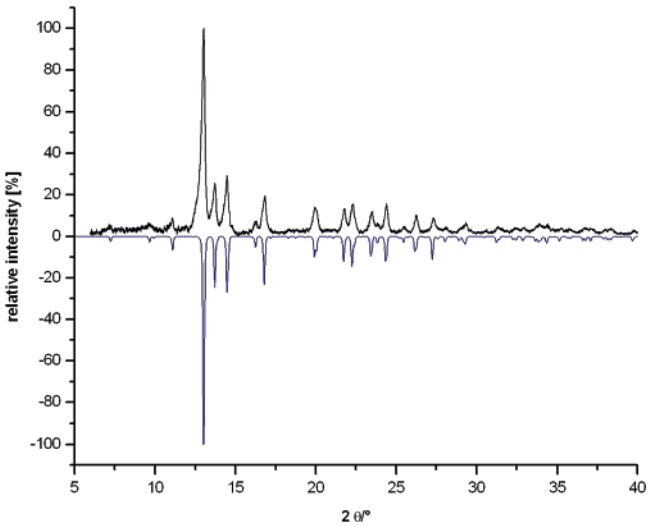

Figure 1. β-Tl_2TeO_3 X-ray powder diffraction pattern: (top) measured data; (bottom) pattern simulated from single-crystal data.

Table 1. Information on Single-Crystal Data Collection and Structure Refinement of α- and β-Tl_2TeO_3[a]

param	β-Tl_2TeO_3	α-Tl_2TeO_3
fw	487.47	487.47
cryst system, space group	*monoclinic*, $P2_1/c$ (No. 14)	*orthorhombic*, *Pban* (No. 50)
Z	4	8
cryst size (mm)	0.2 × 0.1 × 0.6	0.2 × 0.1 × 0.6
wavelength (pm)	71.073	71.073
F(000)	952	1903
θ range for data collcn (deg)	2.4−28.1	2.4−28.1
abs corr	numerical	numerical
refinement method	full-matrix least squares on F^2	full-matrix least squares on F^2

[a] For further information, see the Supporting Information.

Experimental Section

Materials. Thallium carbonate (99.9%, Aldrich), tellurium dioxide (>98%, Merck), and methanol (99.8%, Riedel-de Haën) were used.

Syntheses. Equimolar amounts of Tl_2CO_3 (130 mg) and TeO_2 (44.3 mg) and 0.5 mL of dry methanol were placed in a Pyrex ampule, which was then sealed under vacuum. The reaction mixture was heated to 160 °C for 3 days and subsequently cooled to room temperature at 2 °C/h. The reaction yielded light yellow to brown aggregates of crystals of β-Tl_2TeO_3.

Vibrational Spectroscopy. IR spectra of the solid were recorded using a IFS-66V-S Fourier transform IR spectrometer; samples were ground to a fine powder and pressed in a KBr (MIR region) or a polyethylene matrix (FIR region). Raman spectra were measured with a FRA 106-S Fourier transform Raman spectrometer. The sample was ground to a fine powder and sealed in glass capillaries with an inner diameter of 1 mm and wall thickness of 0.15 mm.

β-Tl_2TeO_3. MIR (cm^{-1}): 833 (w), 775 (w), 752 (w), 704 (m), 654 (m), 623 (s). FIR (cm^{-1}): 343 (s), 308 (s), 286 (s), 203 (m), 185 (m), 163 (m), 111 (w), 101 (w), 93 (m), 85 (m), 74 (m), 56 (w), 45 (w). Raman (cm^{-1}): 708 (s), 646 (m), 346 (w), 296 (m), 150 (m), 117 (m), 93 (m), 66 (w).

Powder X-ray Diffraction. Powder X-ray diffraction data were obtained using an image plate Guinier camera (Huber G670) diffractometer (Mo $K\alpha_1$) (Figure 1).

Crystal Structure Determinations. A few crystals of Tl_2TeO_3 were selected and sealed in thin-walled glass capillaries of 0.3−

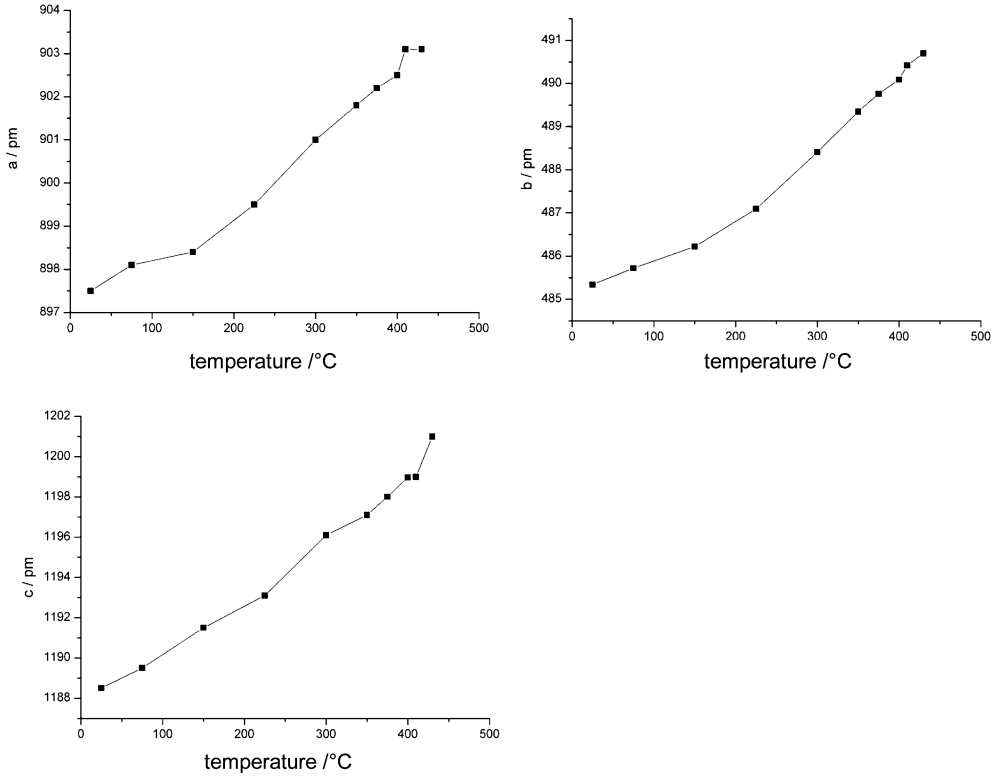

Figure 2. Development of the lattice constants of Tl_2TeO_3 with the temperature (single-crystal data).

Table 2. Lattice Constants of Tl_2TeO_3 (Single-Crystal Data) and Atomic Positions ($\times 10^{-4}$), Wyckoff Symbols, Occupancy, Fractional Coordinates, and Isotropic Displacement Factors (10^{-1} pm^2) for α- and β-Tl_2TeO_3 at 25 °C[a]

cryst	*T*/°C	*a*/Å	*b*/Å	*c*/Å	*β*	*V*/A^3	(*V*/*Z*)/Å^3
β-Tl_2TeO_3	25	8.9752(18)	4.8534(6)	11.884(2)	109.67(2)	487.47(15)	121.87
α-Tl_2TeO_3	25	16.646(2)	11.094(2)	5.2417(8)	90.0	968.0(3)	121.00

atom	Wyck	occ	*x*/*a*	*y*/*b*	*z*/*c*	U_{eq}
			β-Tl_2TeO_3			
Tl1	8*a*	1	5052(1)	2352(2)	8840(1)	30(1)
Tl2	32*e*	1	1894(1)	7322(2)	8133(1)	31(1)
Te	96*g*	1	8323(1)	−2497(2)	9250(1)	24(1)
O1	96*g*	1	6157(14)	−3000(30)	8417(12)	29(2)
O2	96*g*	1	9067(17)	−3030(30)	7985(13)	39(3)
O3	96*g*	1	8296(17)	1350(30)	9261(15)	42(3)
			α-Tl_2TeO_3			
Tl1	8*m*	1	3316(1)	1196(1)	7521(4)	70(1)
Tl2	8*m*	1	4959(1)	1358(1)	2439(5)	66(1)
Te	8*m*	1	6627(1)	1129(2)	7656(5)	53(1)
O1	8*m*	1	3152(12)	515(19)	2830(60)	73(7)
O2	8*m*	1	4433(12)	8980(30)	3150(50)	81(8)
O3	8*m*	1	3447(11)	−1040(30)	−1160(40)	72(8)

[a] Analogous data at other temperatures are given in the Supporting Information.

0.5 mm outer diameter and first were checked by Laue photographs for their quality. The best specimen was used to collect a complete intensity data set with the aid of a single-crystal X-ray diffractometer (Stoe IPDS I using graphite-monochromated Mo Kα X-ray-radiation (λ = 0.701 73 Å)) equipped with a heating stage and a FR559 crystal heater controller (Enraf Nonius). Essential experimental conditions and resulting crystallographic data are summarized in Table 1. The development of the lattice constants with the temperature has been visualized in Figure 2. Fractional atomic coordinates and isotropic displacement factors for both structure types at 25 °C are given in Table 2. Further information is given as Supporting Information and can be downloaded from the Web. Data reduction with the program X-Red[20] in all cases included corrections for background, Lorentz, and polarization effects. A numerical absorption correction with the programs X-Red/X-Shape[21] was undertaken after optimization of the habitus of the crystal. The structures were solved by direct methods with the program SHELXS-97.[22] The atoms were refined anisotropically by a full-matrix least-square procedure using the program SHEXL-

(20) *X-RED*; Stoe & Cie: Darmstadt, Germany, 2002.
(21) *X-Shape*; Stoe & Cie: Darmstadt, Germany, 2002.
(22) Sheldrick, W.S. *SHELXS-97*; Universität Göttingen: Göttingen, Germany, 1997.

Table 3. Selected Interatomic Distances and Angles for α- and β-Tl_2TeO_3 at Room Temperature

β-Tl_2TeO_3				α-Tl_2TeO_3			
dist	*d*/Å	angle	−/deg	dist	*d*/Å	angle	−/deg
Tl1−O1	2.538(25)			Tl1−O1	2.565(20)		
Tl1−O1	2.581(15)			Tl1−O3	2.585(33)		
Tl1−O3	2.825(18)			Tl1−O1	2.587(31)		
Tl1−O1	2.884(15)			Tl1−O1	2.897(31)		
Tl2−O2	2.489(16)			Tl2−O2	2.552(26)		
Tl2−O2	2.612(16)			Tl2−O3	2.760(19)		
Tl2−O3	2.831(19)			Tl2−O2	2.805(32)		
Tl2−O2	2.913(16)						
Te1−O2	1.857(20)	O2−Te1−O3	98.85(68)	Te−O2	1.818(21)	O2−Te−O3	99.41(101)
Te1−O3	1.867(15)	O2−Te1−O1	98.37(64)	Te−O3	1.843(21)	O2−Te−O1	95.43(116)
Te1−O1	1.877(22)	O3−Te1−O1	96.90(67)	Te−O1	1.878(21)	O3−Te−O1	95.53(135)

97.[23] Structure factors were taken from ref 24. For crystal structure drawings, the program Diamond was used.[25]

Computational Details. To analyze the chemical bonding situation in Tl_2TeO_3, calculations on the electronic structure were carried out with the Stuttgarter LMTO-ASA program package which uses the tight-binding linear-muffin-tin orbital (LMTO) method in the local density (LDA) and atomic sphere (ASA) approximation.[26,27] All major relativistic effects except spin-orbit coupling were taken into account using scalar relativistic approximations. The calculations include corrections for the neglect of the interstitial regions and the partial waves of higher order. To reduce the overlap of atomic spheres (AS) empty interstitial spheres were added to the crystal potential and the basis set. The construction of the atomic sphere radii was performed according to an automatic procedure[28] of the program package until the empty space was sufficiently filled.[29] The basis set of short-ranged, atom-centered TB-LMTOs contained *n*s, *n*p, *n*d, and $(n-1)$f wave functions for Tl ($n = 6$) and Te ($n = 5$). The d and f waves were included only in the tails of the LMTOs according to the Löwdin downfolding procedure.[30] For oxygen 2p was taken fully into account while 3s and 3d functions were downfolded.

All reciprocal space integrations are carried out using the tetrahedron method.[31] To examine in detail the effect of the anion on the electronic density of states, the partial-ion *l* and *m* quantum number decomposed electronic density of states has been calculated. They were calculated by projecting the wave functions onto spherical harmonics centered on each atom (PDOS = projected density of states). For bond analysis the crystal orbital Hamiltonian population (COHP) method is used together with its integration, the ICOHP.[32]

In all cases the structural data were employed as gained from single-crystal X-ray data. The highest occupied level is always chosen as the level of reference for the energy.

Results and Discussion

Crystal Structure. It has been recently shown that conventional solid-state reactions as well as hydrothermal routes are viable for the synthesis of tellurites.[33] Under methanolothermal conditions (see Experimental Section) a new modification of Tl_2TeO_3 has been obtained from Tl_2CO_3 and TeO_2. Being a thermodynamically unstable modification, this compound has been so far missed in studies of the Tl_2O/TeO_2 system.[34] In contrast to the already known orthorhombic high-temperature modification[35] obtained by conventional high-temperature synthesis, β-Tl_2TeO_3 crystallizes monoclinic with the space group $P2_1/c$. The structure is characterized by ψ-tetrahedral TeO_3^{2-} complex anions with a mean Tl−O distance of 1.87 Å (25 °C) and an average −O−Te−O angle of 98° (Table 3).

Thallium is found in the form of ψ-square pyramidal [TlO_4] units. Each [TlO_4] unit is connecting to three [TeO_3] pseudotetrahedral units so that corrugated layers perpendicular to the crystallographic *c*-axis are formed (Figure 3).

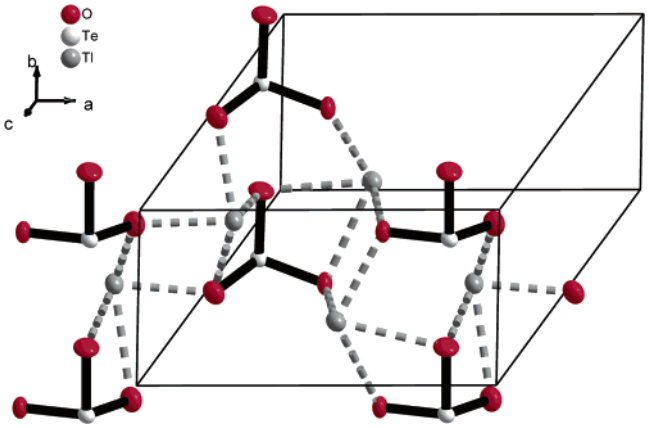

Figure 3. Crystal structure of β-Tl_2TeO_3. Corrugated layers in the $a-b$ plane are formed by [TeO_3] and [TlO_4] units.

(23) Sheldrick, W.S. *SHELXL-97*; Universität Göttingen: Göttingen, Germany, 1997.
(24) Prince E., Ed. *International Tables for Crystallography*; Kluwer Academic Publishers: Dortrecht, Germany, 2004; Vol. C.
(25) *Diamond*, ver. 2.1; Crystal Impact GbR: Bonn, 1998.
(26) Shriver, H. L. *The LMTO Method*; Springer-Verlag: Berlin, Germany, 1984. Jepsen, O.; Snob, M.; Andersen, O. K. *Linearized Band-Structure Methods in Electronic Band-Structure and its Applications*; Springer Lecture Note; Springer-Verlag: Berlin, Germany, 1987. Anderson, O. K.; Jepsen, O. *Phys. Rev. Lett.* **1984**, *53*, 2571.
(27) Tank, R. W.; Jepsen, O.; Burckhardt, A.; Andersen, O. K. *TB-LMTO-ASA Program*, vers. 4.7; Max-Planck-Institut für Festkörperforschung: Stuttgart, Germany, 1998.
(28) Jepsen, O.; Anderson, O. K. *Z. Phys.* **1995**, *B97*, 35.
(29) The automatic routine yielded in the case of the monoclinic structure for Tl1 a radius of 4.13 for Tl1, 4.02 for Tl2, 2.74 for Te, 1.58 for O1, 1.59 for O2, and 1.57 Å for O3. For the orthorhombic structure radii of 3.83 for Tl1, 3.99 for Tl2, 2.60 for Te, 1.70 for O1, 1.89 for O2, and 1.79 Å for O3 were generated. The muffin tin radii for the empty spheres ranged from ∼2 to ∼1 Å. Special care was taken to choose comparable ASA radii for both structures to allow for a better comparison.
(30) Lambrecht, W. R. L.; Andersen, O. K. *Phys. Rev. B* **1986**, *B34*, 2439. Jensen, O. Andersen, O. K. *Z. Phys. B.* **1995**, *B97*, 35. Krier, G.; Jepsen, O.; Andersen, O. K. Max-Planck-Institute fur Festkörperforschung, Stuttgart, Germany, unpublished.
(31) Andersen, O. K.; Jepsen, O. *Solid State Commun.* **1971**, *9*, 1763. Blöchl, P.; Jepsen, O.; Andersen, O. K. *Phys. Rev. B.* **1994**, *34*, 16223.

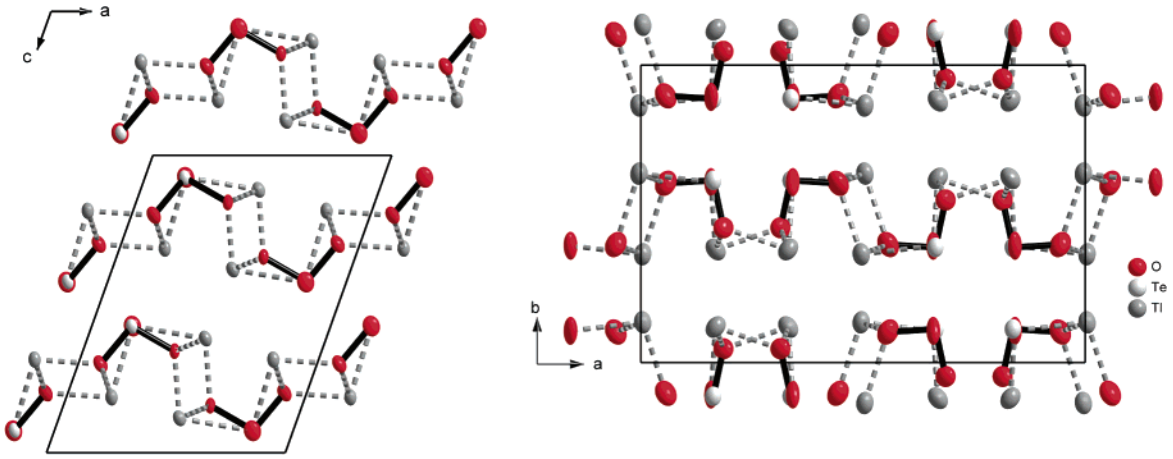

Figure 4. Comparison of the crystal structures of β-Tl_2TeO_3 (left) and β-Tl_2TeO_3 (right). The phase transition is basically achieved by a pairwise clockwise−counterclockwise motion of the [TeO_3] units against each other.

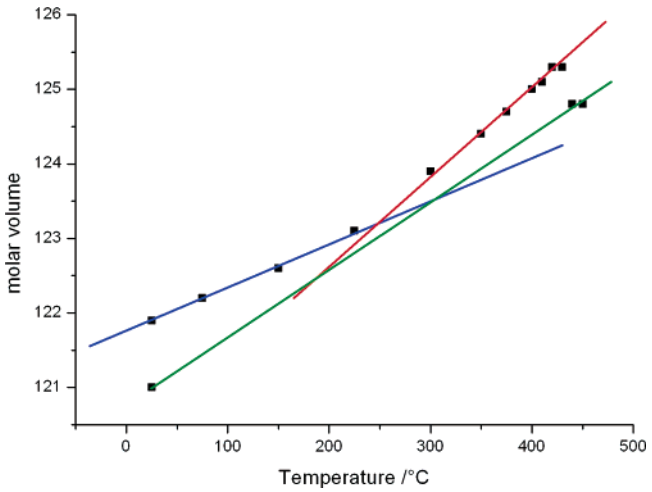

Figure 5. Evolution of the molar volume in Å^3 of Tl_2TeO_3 with the temperature.

The mean Tl−O distance within the ψ-square pyramidal [TlO_4] unit is 2.71 Å with two shorter and two larger Tl−O contacts (Table 3). One of the two crystallographically independent thallium cations (Tl2) is connecting the single layers via a Tl−O contact of 3.22(2) Å parallel to the *c*-axis (Table 3) to a three-dimensional extended network structure. Thus, the surrounding of Tl2 can be regarded as a 4 + 1 coordination in the form of a ψ-octahedron by oxygen atoms.

The transition to the higher symmetrical orthorhombic structure is basically achieved by a pairwise clockwise−counterclockwise motion of the [TeO_3] units against each other (Figure 4).

By this, the layered structure of Tl_2TeO_3 is essentially retained (Figure 5). In the pseudotetrahedral [TeO_3] units of α-Tl_2TeO_3 the Te−O distances becomes slightly less uniform (Table 3). The mean Te−O interatomic distance drops to 1.84 Å, and the mean O−Te−O angles goes down to 96.8°.

The most important change occurs in the coordination spheres of the thallium cations. On the one hand, the mean Tl−O interatomic distance of Tl−O contacts below 3 Å amounts to 2.68 Å, which is about 0.03 Å less than observed for the monoclinic structure at the same temperature. At the same time, the coordination environment of thallium changes rather dramatically. While the coordination number for one thallium remains 4, the coordination polyhedron is better described by a ψ-trigonal pyramid than a ψ-square pyramid. For the other crystallographically independent thallium cation the most pronounced change is observed. While below 3 Å just three Tl−O contacts are observed (Table 3), three more oxide anions are found at distances of 3.10(3), 3.12(3), and 3.16(2) Å which complete the coordination sphere of this cation to what probably can be best described as a ψ-pentagonal pyramid of oxygen.

In consequence, more Tl−O contacts and, thus, a larger thallium-oxygen interaction are present in the (higher symmetric) orthorhombic structure than in the monoclinic structure. The larger thallium−oxygen interaction is reflected by the evolution of the molar volume with the temperature where a sudden drop of the molar volume is observed at 440 °C (Figure 5). From Figure 5 it also becomes clear that the molar volume decreases not linearly with the temperature. Rather the temperature dependent change of the molar volume of the monoclinic phase can be described by two linear fits in the temperature range from room temperature to about ∼250 °C and from there to the phase transition temperature (∼440 °C). At a temperature of 510 °C melting of β-Tl_2TeO_3 is observed.[36] The phase transition from the monoclinic to the orthorhombic structure is monotropic. Even upon slow cooling the orthorhombic structure was preserved.

(32) Dronskowski, R.; Blöchl, P. E. *J. Phys. Chem.* **1993**, *97*, 8617.
(33) Minimol, M. P.; Vidyasagar, K. *Inorg. Chem.* **2005**, *44*, 9369.
(34) Jeannesannetas, B.; Marchet, P.; Thomas, P.; Champarnaud-Mesjard, J. C.; Frit, B. *J. Mater. Chem.* **1998**, *8*, 1039.
(35) Frit, B.; Mercurio, D. *Rev. Chim. Miner.* **1980**, *17*, 192. Frit, B.; Mercurio, D.; Thomas, P.; Champarnaud-Mesjard, J.C. *Z. Kristallogr. New Cryst. Struct.* **1999**, *214*, 439.
(36) DSC measurement show a melting point of 380 °C. We attribute this lower melting point to mechanically induced changes (like, e.g., observed in the case of SiO_2 for tridymite: Cellai, D.; Carpenter, M. A.; Kirkpatrick, R. J.; Salje, E. K. H.; Zhang, M. *Phys. Chem. Miner.* **1995**, 50). After cooling, α-Tl_2TeO_3 crystallizes from the melt. Interestingly the observed melting point of 380 °C corresponds well to previously reported (incongruent) melting point of the α-modification of Tl_2TeO_3 (Jeannesannetas, B.; Marchet, P.; Thomas, P.; Champarnaud-Mesjard, J. C.; Frit, B. *J. Mater. Chem.* **1998**, *8*, 1039). α-Tl_2TeO_3 crystallizes from the melt.

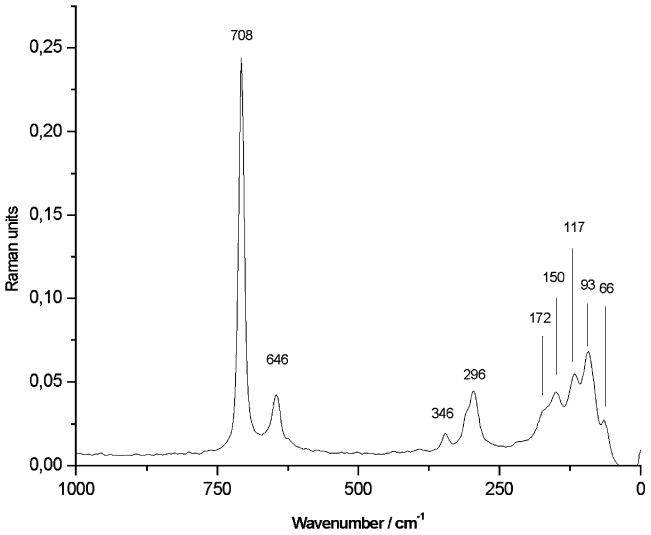

Figure 6. Raman spectrum of β-Tl_2TeO_3.

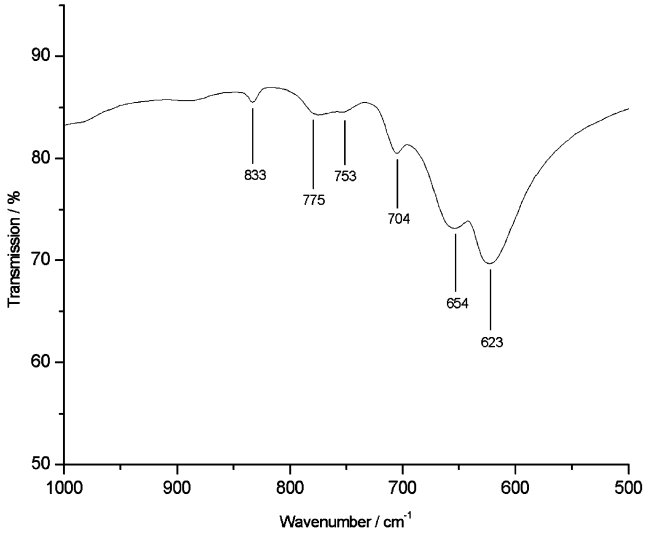

Figure 7. MIR spectrum of β-Tl_2TeO_3.

Infrared and Raman Spectroscopy. As the TeO_3^{2-} anion has approximately C_{3v} symmetry, its stretching and bending vibrations can be described in a first approximation as the $A_1 + E$ ones of a pyramid-like molecule. The TeO_3^{2-} anion is expected to give rise to a symmetric and an asymmetric Te−O stretching vibration. Indeed, these can be found at wavenumbers of 707.6 and 645.8 cm^{-1} in the Raman spectrum (Figure 6). The first band corresponds to a mode with approximately A_1 symmetry; the latter one, to the E modes. The corresponding spectral region is displayed in the MIR spectrum in Figure 7. The broad bands found in the far-infrared spectrum (Figure 8) of β-Tl_2TeO_3 at wavenumbers between 350 and 280 cm^{-1} (343, 308, and 286 cm^{-1}; Figure 8) can be attributed to O−Te−O bending vibrations. The Raman spectrum (Figure 6) shows in this region two bands at 345.9 and 295.6 cm^{-1}, respectively. Bands found in the region between 120 and 200 cm^{-1} can be associated with Tl−O modes, whereas at even lower wavenumbers the vibrations most probably stem from interpyramidal O−O interactions. The vibrational spectra of α-Tl_2TeO_3 have been

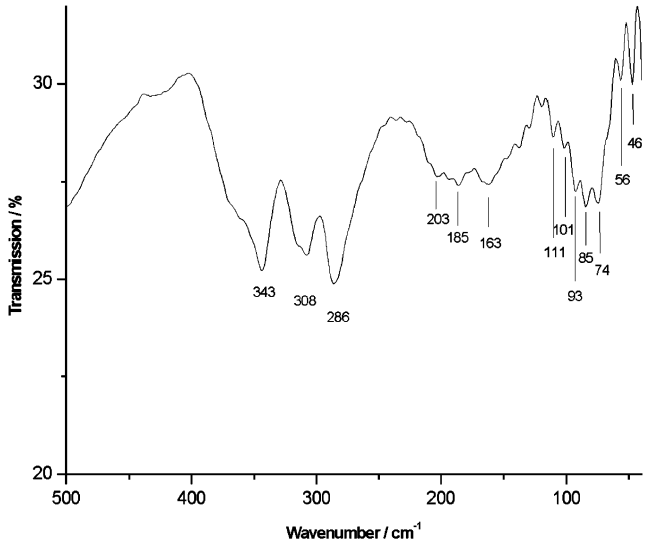

Figure 8. FIR spectrum of β-Tl_2TeO_3.

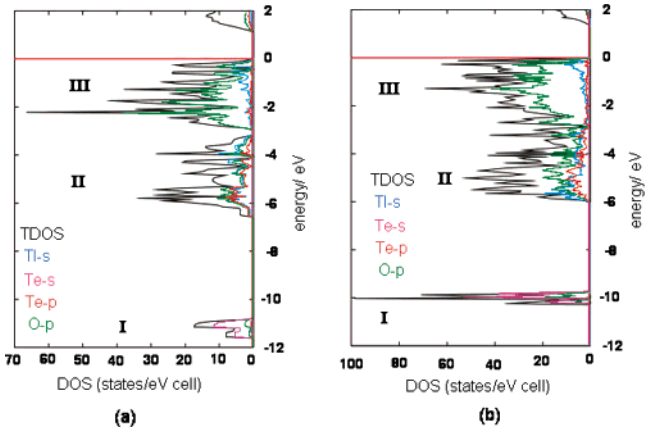

Figure 9. DOS and PDOS of α- (left) and β-Tl_2TeO_3 (right).

extensively studied previously.[37] Although the general features of the spectra are the same, two major differences are noteworthy. First, due to the lower local symmetry of the TeO_3^{2-} anion (stronger deviation from the idealized C_{3v} symmetry) the bands in the region between 750 and 600 cm^{-1} are split, and second, due to the change of the thallium surroundings the bands at ∼100 and 150 cm^{-1} are broadened in the spectrum of α-Tl_2TeO_3.

Theory. The density of states of both α- and β- Tl_2TeO_3 calculated within the framework of density functional theory shows overall the same features. At the lowest (displayed) energies a region (I) formed by mainly Te-s states with some O-p contribution is found (Figure 9). The broad region at higher energies following extends up to the Fermi level and shows contributions mainly by O-p but also by Tl-s and Te-p states. This region is divided by a pseudogap which also separates two different regions (II and III).

Whereas the region at energies between ∼−5.5 and −3 eV (II) is formed by roughly equal contributions of O-p, Tl-

(37) Dexpert-Ghys, J.; Piriou, B.; Rossignol, S.; Reau, J. M.; Tanguy, B.; Videau, J. J.; Portier, J. *J. Non-Cryst. Solids* **1994**, *170*, 167. Tekiya, T.; Mochida, N.; Ohtsuka, A.; Tonokawa, M. *J. Non-Cryst. Solids* **1992**, *144*, 128. Mirgorodsky, A. P.; Merle-Méjean, T.; Thomas, P.; Champarnaud-Mesjard, J. C.; Frit, B. *J. Phys. Chem. Solids* **2002**, *63*, 545.

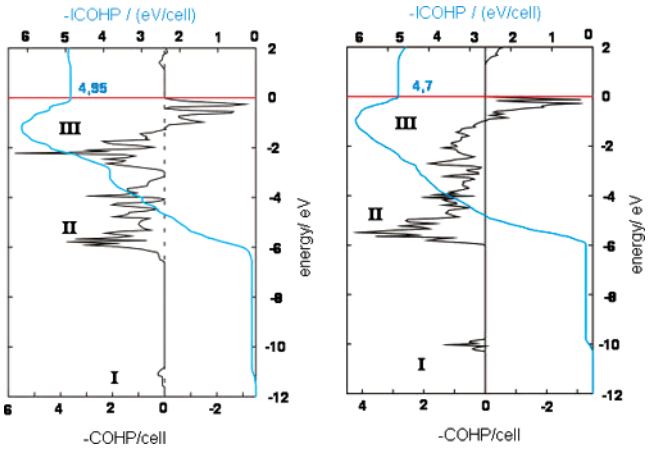

Figure 10. (I)COHP for the Tl−O band in α- (left) and β-Tl_2TeO_3 (right).

s, and Te-p states in the region from −3 eV up to the Fermi level (III), the contribution of Te-p states becomes negligible. Instead, this region is dominated by O-p states with Tl-s states becoming important close to the Fermi level. A closer inspection of the chemical bonding by means of the crystal orbital Hamiltonian population (COHP) analysis in both modifications of Tl_2TeO_3 reveals some rather distinct differences.

Whereas region II is totally Tl−O bonding, region III can now be subdivided into two sections. The lower part of region III is Tl−O bonding in contrast to the upper part which is Tl−O *anti*bonding. Integration of the bonding interaction (ICOHP = integrated crystal orbital Hamiltonian population) from low energies to the Fermi level shows in case of monoclinic β-Tl_2TeO_3 a larger net bonding interaction than for α-Tl_2TeO_3 (4.95 vs 4.7 eV/cell) (Figure 10). Hence, it can be deduced that as it has been previously described for thallium complexes[38] and thallous halides[39] that structural distortions ascribed to the lone pair of thallium originate from the tendency to minimize antibonding interactions of the thallium $6s^2$ lone pair with its surrounding.

Similar theoretical calculations on the analogous thiotellurite can explain why thallium adopts in Tl_2TeS_3,[40] in contrast to Tl_2TeO_3, a comparatively highly symmetric surrounding. The considerably lower degree of distortion in the sulfur compound is due to the energetical mismatch of the 6s-Tl and 3p-S states. The 6s-Tl orbitals are shifted downward in energy by relativistic effects, and therefore, their separation on the energy scale from the 3p-S states is fairly large leading only to a comparatively weak covalent interaction. Thus, the minimization of antibonding 6s-Tl/3p-S lone pair interactions by structural distortions is less favored. Instead, a higher symmetric structure with a larger Madelung energy, hence, Coulombic interactions is obviously preferred.

Conclusions

It is well-established that many interesting material's properties can be expected from compounds that contain building units that have a high dipolar character—like for example in Tl_2TeO_3 or in Tl_2O/TeO_2 glasses. One strategy is to use chemical entities which possess a stereochemically active lone pair. Unfortunately, although a large number of rules of thumb exist, little is known about the true nature of such stereochemically active lone pairs. By investigation of the phase transition of Tl_2TeO_3, it can be shown that the minimization of unfavorable Tl-$6s^2$/O-$2p^6$ interactions which take place right at the Fermi level are the driving force for such lone pair distortions. Comparison with Tl_2TeS_3 shows that such Tl-$6s^2$/S-$2p^6$ interactions play a minor role due to the energetical mismatch of the involved orbitals. Generalization of this observation might explain why in compounds with softer ligands or counteranions lone pair distortions are less likely to be observed and it can be deduced that (and why) structures with highly dipolar groups are best constructed by two partners which contain closed-shell ions that have in energetical terms matching orbitals.

Acknowledgment. A.-V.M. thanks the BMBF and Fonds der Chemischen Industrie for support and the Deutsche Forschungsgemeinschaft for generous financial support. Prof. Dr. G. Meyer is acknowledged for his interest in this research, for the discussions, and for the provision of the necessary infrastructure to conduct this research.

Supporting Information Available: This material is available free of charge via the Internet at http://pubs.acs.org.

IC061273J

(38) Mudring, A. V.; Rieger, F. *Inorg. Chem.* **2005**, *44*, 6240.
(39) Mudring A.-V. In *Inorganic Chemistry in Focus III*; Meyer, G., Naumann, D., Wesemann, L., Eds.; 2006. Mudring, A. V. *Eur. J. Inorg. Chem.* **2006**, in press.
(40) Rieger, F.; Mudring, A. V. *Chem. Mater.* **2007**, in press.